DIFFERENCE SYSTEM AND BOUNDARY CONDITIONS FOR THE PRIMITIVE-EQUATION BAROTROPIC FORECAST

FREDERICK G. SHUMAN AND LLOYD W. VANDERMAN
National Meteorological Center, Weather Bureau, ESSA, Washington, D.C.

ABSTRACT

A primitive-equation free-surface barotropic model was designed for the tropical belt. By the use of Shuman's difference system, experiments were made to test the effect of both approximate and correct boundary conditions on the forecast fields. Results are shown in the figures. With the correct boundary conditions a successful forecast was calculated without smoothing to 100 days.

1. INTRODUCTION

At the National Meterological Center (NMC) we are developing a system for short-range large-scale forecasting in the Tropics. It is being done as a part of our responsibility as the analysis-forecast arm of the World Weather Center (Washington), established in December 1964. The system consists of acquisition of data, computer-processing of data, numerical weather analysis, and numerical weather prediction. The present paper deals with the prediction model, and particularly emphasizes its viability in long-term integrations.

The model was not designed with such viability in mind. With the basic model developed, however, it was a great temptation to determine its stability characteristics, for it is an inexpensive model to run on a computer. Although the numerical system used has long since been reported [1], it has remained obscure, being only occasionally referenced by writers dealing with long-term integrations, and never to the writers' knowledge tested or used in extended integrations. At NMC we have been using the numerical system for over six years now, but only for short-range predictions. The earlier work [1], however, contains strong indications that the numerical system should be stable in extended calculations, because of the extreme initial conditions on which it was tested.

2. FORECAST MODEL

A primitive-equation free-surface barotropic forecast model was designed for a Mercator projection of the tropical belt. A 5°-longitude grid was employed. Rigid walls along latitude circles were placed at approximately 46° N. and S. East and west ends of the forecast grid completed the tropical belt and were cycled, thereby making the fields continuous in the east-west directions. A difference system reported by Shuman [1] was employed throughout. Initial conditions consisted mainly of wave number three superimposed on an easterly jet, although components other than wave number three were present. Test forecasts with different boundary conditions consistent with the difference system were calculated. It was found that approximate boundary conditions create gravity waves and that a successful long-period forecast requires boundary conditions consistent with the physical model. Employing the latter we ran the forecast to 100 days in 10-min. time steps. Neither smoothing nor viscosity was employed to control the calculation, nor have the results presented here been smoothed.

The differential equations describing the mechanics of the model, in Cartesian coordinates on a Mercator projection are:

$$\frac{\partial u}{\partial t}-fv+m\left(u\frac{\partial u}{\partial x}+v\frac{\partial u}{\partial y}+\frac{\partial gh}{\partial x}\right)=0 \tag{1.1}$$

$$\frac{\partial v}{\partial t}+fu+m\left(u\frac{\partial v}{\partial x}+v\frac{\partial v}{\partial y}+\frac{\partial gh}{\partial y}\right)=0 \tag{1.2}$$

$$\frac{\partial h}{\partial t}+m\left[u\frac{\partial h}{\partial x}+v\frac{\partial h}{\partial y}+h\left(\frac{\partial u}{\partial x}+\frac{\partial v}{\partial y}\right)\right]-hv\frac{\partial m}{\partial y}=0 \tag{1.3}$$

where x, y, and t are the independent space-time coordinate variables; f the Coriolis parameter; g the acceleration of gravity; u and v the eastward and northward velocity components, respectively; h the height of the free surface; and m the map scale factor, which for the Mercator projection equals the secant of the latitude.

For convenience in writing the finite-difference analogs to the above equations, we adopt notations described in the earlier paper [1]. For example, if grid points are numbered serially with increasing x along a line of constant y and t, as 0, 1, 2, . . . $i-1$, i, $i+1$, . . . , then

$$u_x\equiv\frac{1}{\Delta x}\left(u_{i+1/2}-u_{i-1/2}\right) \tag{2.1}$$

$$\overline{u}^x\equiv\tfrac{1}{2}\left(u_{i+1/2}+u_{i-1/2}\right) \tag{2.2}$$

with similar symbolism holding for other functions of the independent variables and for the other independent variables.

Attachment of additional subscripts or superscripts has the following meaning:

$$u_{xx}=(u_x)_x \tag{3.1}$$

$$\overline{u}^{xx}=(\overline{u^x})^x. \tag{3.2}$$

Now consider the equations for one-dimensional gravity waves in a homogeneous incompressible layer with variations in one space dimension only.

$$\frac{\partial u}{\partial t}+u\frac{\partial u}{\partial x}+\frac{\partial gh}{\partial x}=0 \tag{4.1}$$

$$\frac{\partial h}{\partial t}+u\frac{\partial h}{\partial x}+h\frac{\partial u}{\partial x}=0 \tag{4.2}$$

The finite-difference analog which Shuman called "semi-momentum" is

$$\overline{u}^t_t+\tfrac{1}{2}\overline{(u^2)}^x_x+g\overline{h}^x_x=0 \tag{5.1}$$

$$\overline{h}^t_t+\overline{(hu)}^x_x=0. \tag{5.2}$$

For purposes of generalization to two space dimensions, we note that these may be written

$$\overline{u}^t_t+\overline{(\overline{u}^x u_x+gh_x)}^x=0 \tag{6.1}$$

$$\overline{h}^t_t+\overline{(\overline{u}^x h_x+\overline{h}^x u_x)}^x=0 \tag{6.2}$$

which amount to first estimates of the tendencies between grid points, which are then averaged to obtain the tendencies at grid points. Applying this principle to our two-dimensional problem (equation (1)) leads to:

$$\overline{u}^t_t+\overline{[-\overline{f}^{xy}\overline{v}^{xy}+\overline{m}^{xy}(\overline{u}^{xy}\overline{u}^y_x+\overline{v}^{xy}\overline{u}^x_y+g\overline{h}^y_x)]}^{xy}=0 \tag{7.1}$$

$$\overline{v}^t_t+\overline{[\overline{f}^{xy}\overline{u}^{xy}+\overline{m}^{xy}(\overline{u}^{xy}\overline{v}^y_x+\overline{v}^{xy}\overline{v}^x_y+g\overline{h}^x_y)]}^{xy}=0 \tag{7.2}$$

$$\overline{h}^t_t+\overline{\{-\overline{h}^{xy}\overline{v}^{xy}\overline{m}^x_y+\overline{m}^{xy}[\overline{u}^{xy}\overline{h}^y_x+\overline{v}^{xy}\overline{h}^x_y+\overline{h}^{xy}(\overline{u}^y_x+\overline{v}^x_y)]\}}^{xy}=0. \tag{7.3}$$

These are the finite-difference analogs used for the present study. Note that the map scale factor, m, and the Coriolis parameter, f, vary with y only so that the $\overline{(\ )}^x$ operation on m and f has no effect, that is

$$\overline{m}^x=m \tag{8.1}$$

and likewise

$$\overline{f}^x=f. \tag{8.2}$$

The u and v wind components were the initial data. The initial height field was obtained by solving the balance equation for h,

$$[\overline{h}^{yy}_{xx}+\overline{h}^{xx}_{yy}]=-\frac{1}{g}\overline{\left[\overline{u}^{xy}\overline{u}^y_x+\overline{v}^{xy}\overline{u}^x_y-\frac{\overline{v}^{xy}\overline{f}^y}{\overline{m}^y}\right]}^y_x-\frac{1}{g}\overline{\left[\overline{u}^{xy}\overline{v}^y_x+\overline{v}^{xy}\overline{v}^x_y+\frac{\overline{u}^{xy}\overline{f}^y}{\overline{m}^y}\right]}^x_y. \tag{9.1}$$

Before solving for h, the right-hand values of equation (9.1) were normalized for two distinct sets of points to avoid the separation of solutions at alternate points allowed by the finite-difference form. Inflow-outflow at the wall was made equal to zero by applying initially the condition of equation (11.2). During the relaxation in solving equation (9.1) the boundary was allowed to float (the boundary condition in the Neumann Problem) by the imposition of geostrophic flow at the wall after each scan, according to equation (11.3). Considerations in solving for h were as involved as those in deducing the correct boundary conditions for the forecast equations. In the calculations, $\Delta x=\Delta y=555.55$ km. (5° of longitude at the equator), $\Delta t=10$ min., and the mean value of h was 2500 m. Central time differences were taken after the first time step, which was forward.

3. BOUNDARY CONDITIONS

One set of boundary conditions applied at the northern and southern walls (halfway between the outermost and the first interior grid rows) of a channel are:

$$u_y=0 \tag{10.1}$$

$$\overline{v}^y=0 \tag{10.2}$$

$$h_y=0. \tag{10.3}$$

In application u and h on the outermost grid row are made equal to values, respectively, at adjacent points on the first interior grid row. The v on the outermost grid row is set equal to the negative of v at the adjacent point on the first interior grid row. The philosophy behind the use of these as boundary conditions was that they provide for reflection of pure gravity waves at the wall. It was reasoned that the inertial effects (due to the presence of f in the equations) on the gravitational oscillations acted much more slowly than the gravitational oscillations themselves, and that, therefore, in attempting to provide a set of boundary conditions innocuous to the calculations, the inertial effects could be ignored, at least for a limited time. As we shall see, this reasoning contained much of truth, but the time limit during which inertial effects at the wall could be ignored turned out to be only a few days. These boundary conditions produced gravity waves in the forecast which "blew up" starting at about 13 days (see

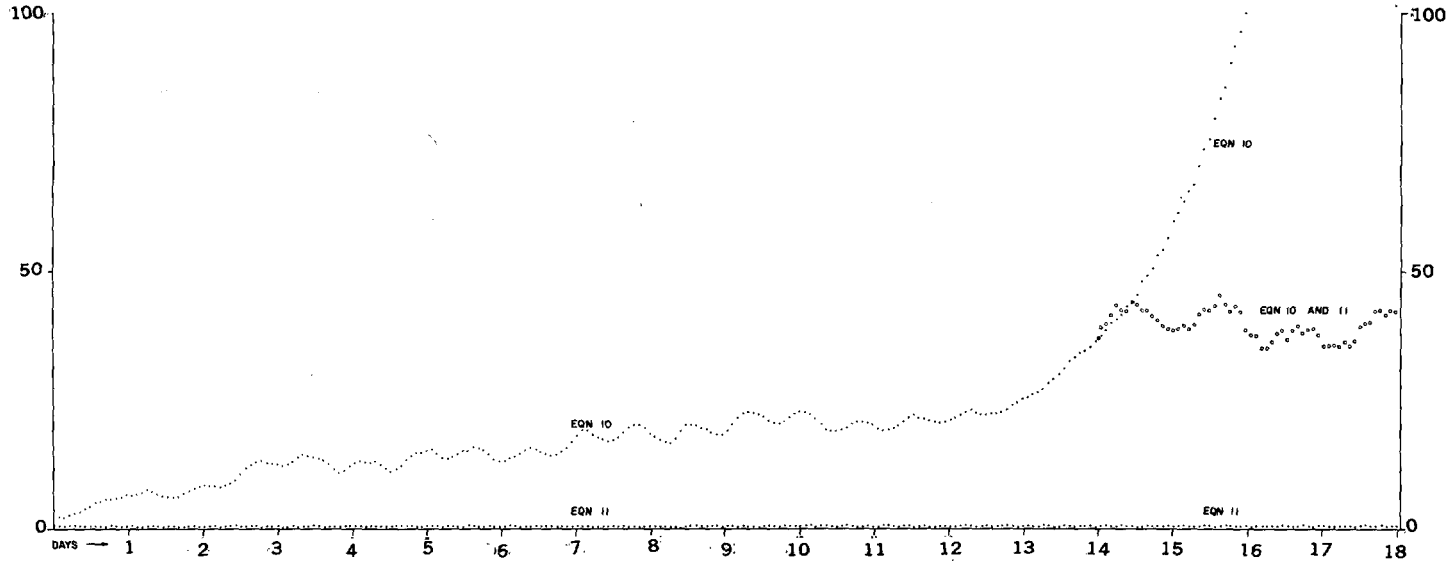

FIGURE 1.—Root-mean-square divergence (ordinate, units times 10^{-6} sec.$^{-1}$; abscissa, time in days) values plotted for ten time-step (100 min.) intervals for the boundary condition equations indicated by the labels of the curves.

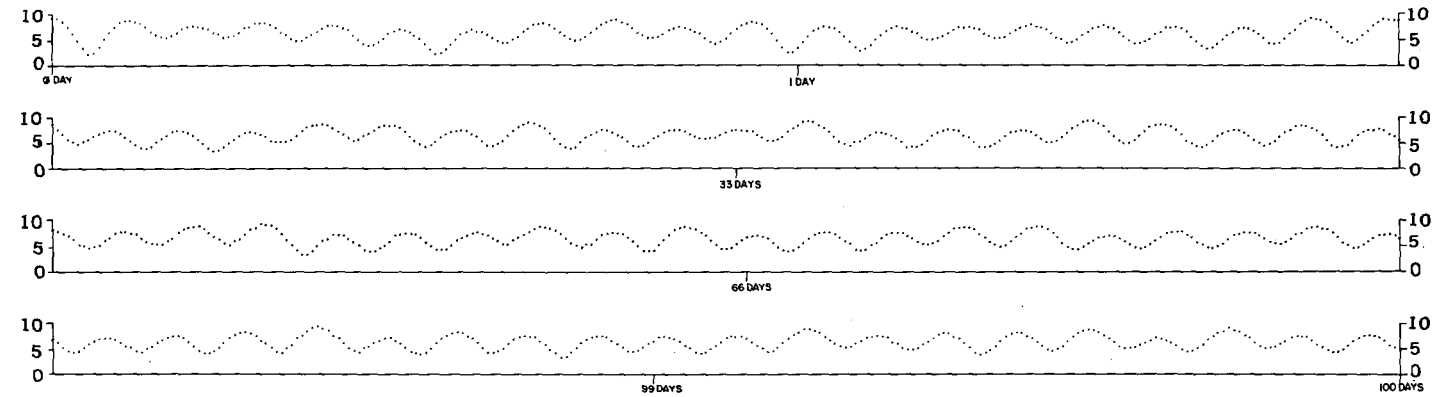

FIGURE 2.—Root-mean-square divergence (ordinate, units times 10^{-7} sec.$^{-1}$; abscissa, time in days) values plotted for each time-step (10 min.) for boundary conditions of equation (11). Each plot is for nearly a 2-day period and from top to bottom they are centered approximately on 1, 33, 66, and 99 days, respectively.

fig. 1). Although these conditions contain obvious inconsistencies, their simplicity of application provided an added incentive to try them. The correct boundary conditions are:

$$\overline{u}^{ty}_{t}+\overline{\overline{m}^{y}\left(\overline{u}^{xy}\overline{u}^{y}_{x}+g\overline{h}^{y}_{x}\right)}^{x}=0 \qquad (11.1)$$

$$\overline{v}^{y}=0 \qquad (11.2)$$

$$\overline{f}^{y}\overline{u}^{y}+\overline{m}^{y}gh_{y}=0. \qquad (11.3)$$

Equation (11.1) is applied to the u tendency field. Equation (11.2) is applied to the v field and insures no flow through the wall at any point. Equation (11.3) is applied to the h field and insures geostrophic flow along the wall.

4. FORECAST RESULTS

Applying the boundary conditions of equation (11), and using the wave number three initial flow we calculated a forecast without smoothing to 100 days. (See figs. 2 to 6.) The u, v, and h fields were printed initially and thereafter at each 12-hr. interval of the forecast. Several years of

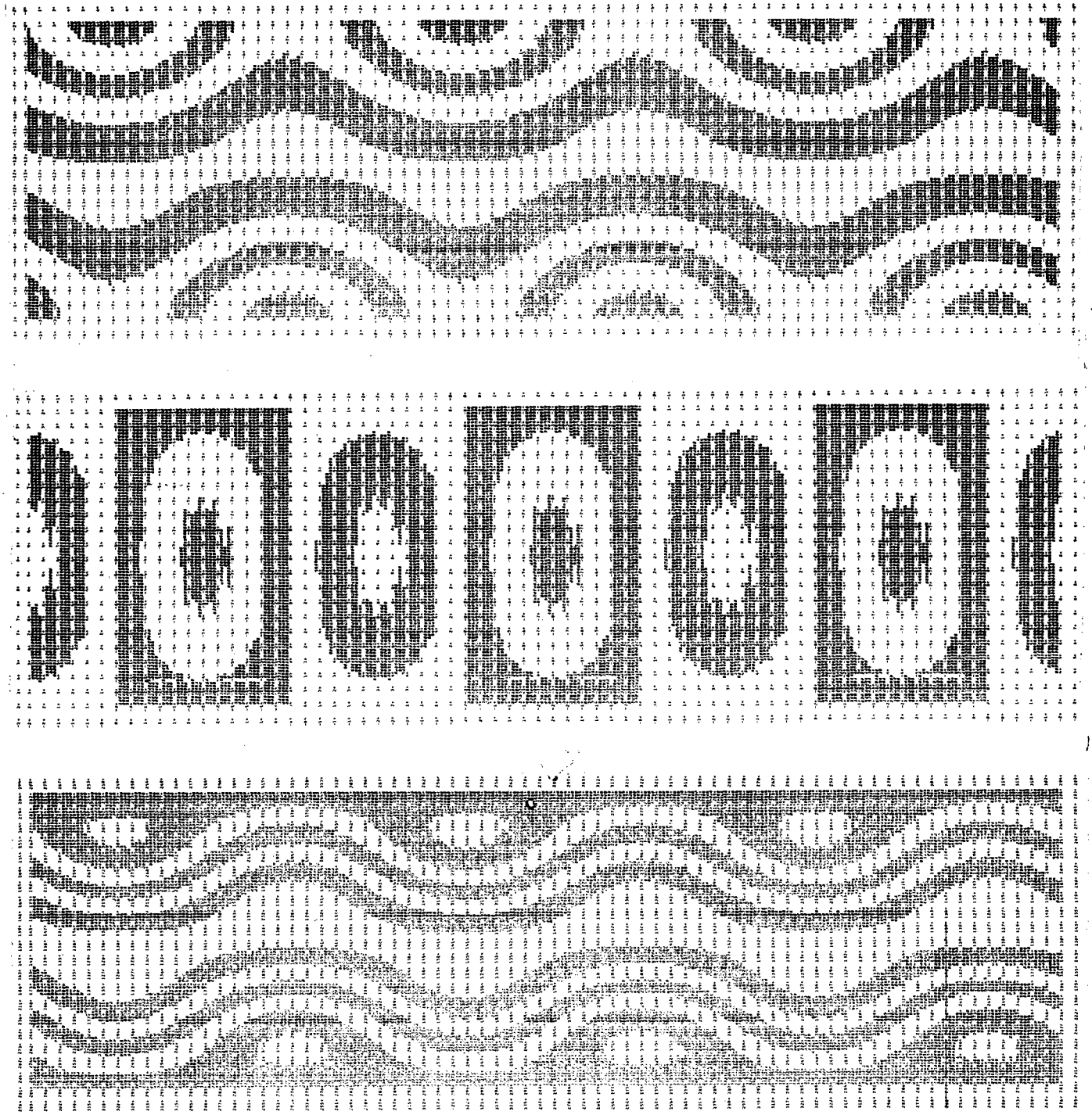

FIGURE 3.—Top, middle, and bottom maps are the initial u, v, and h fields, respectively.

experience have shown us that the most sensitive indicator of computational instability is not one of the quantities which the hydrostatic differential equations conserve but, rather, the behavior of the vertical velocity (or divergence, which is closely related). For this reason, time-charts of RMS divergence have been chosen for display in figures 1 and 2. Figure 2 shows the perfect stability of the calculation with the correct boundary condition. Root-mean-square divergence had a small value initially, remained small throughout the 100-day period, and

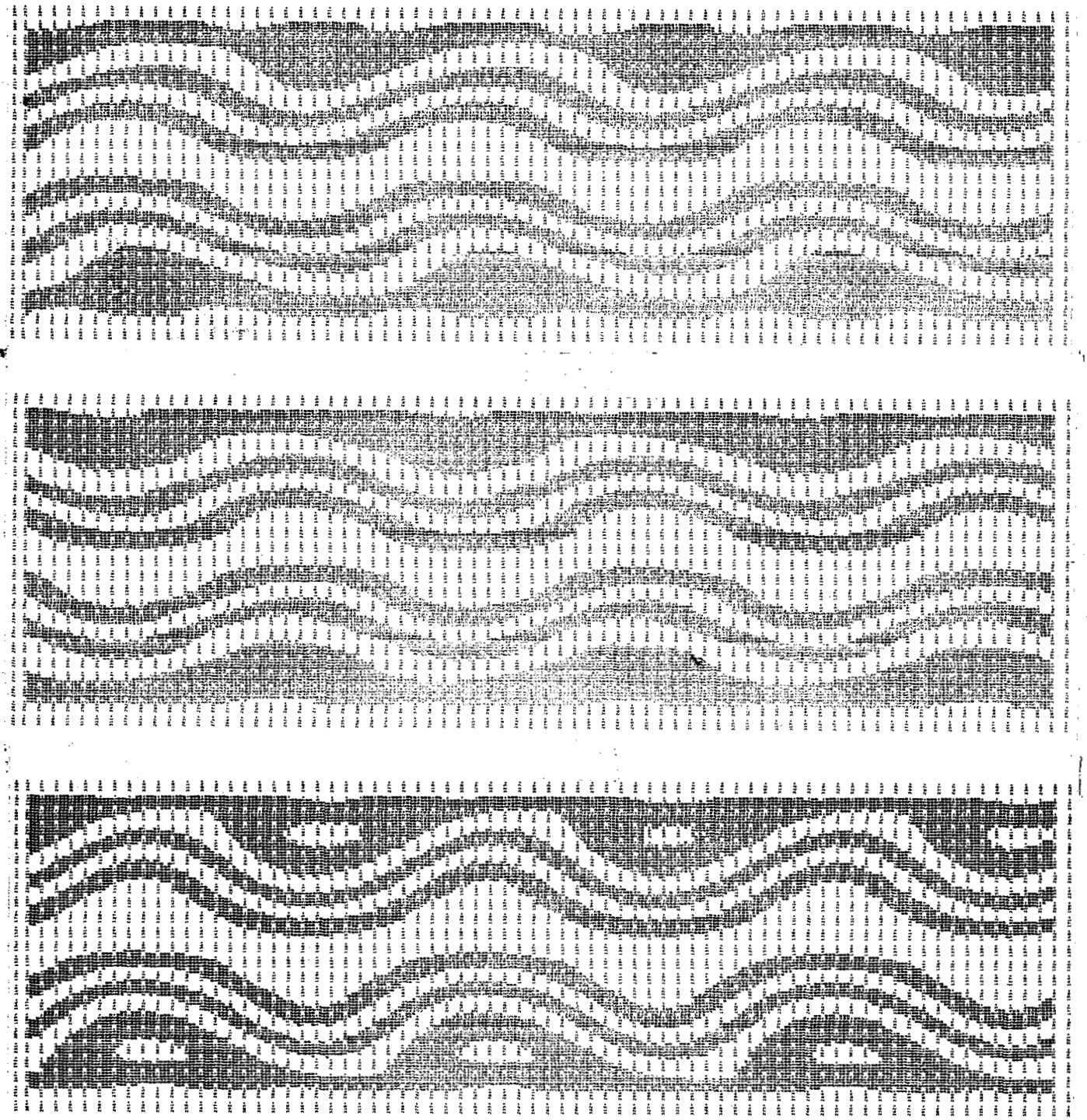

FIGURE 4.—Top, middle, and bottom maps are the 1-day, 2-day, and 3-day forecast h fields, respectively.

varied with a cycle of approximately 13 time steps (2 hr., 10 min.). Mean height was calculated also at each time step and varied no more than 1 m. throughout the 100 days. As an interesting side experiment the forecast that started "blowing up" at 13 days was continued on from 14 days with the correct boundary conditions of equation (11). Values of root-mean-square divergence (see fig. 1) from this experiment indicated no further deterioration of the forecast.

The most interesting forecast fields are of height, shown

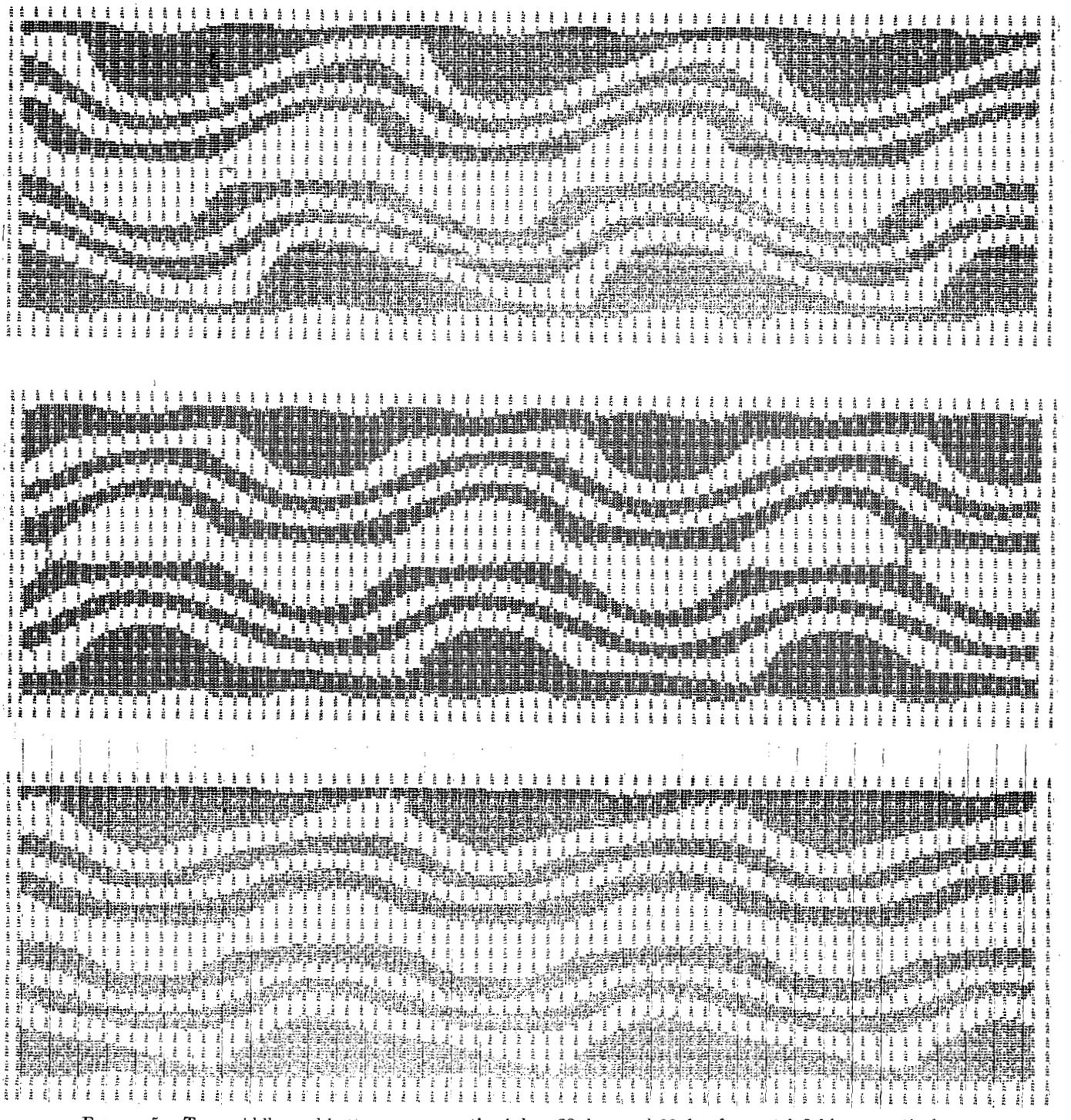

FIGURE 5.—Top, middle, and bottom maps are the 4-day, 33-day, and 66-day forecast h fields, respectively.

in figures 3 to 6. In the basic easterly flow the systems move westward slightly faster than the Rossby speed in reasonable agreement with linear theory of displacement. The high-latitude anticyclones decay and regenerate; the waves start to occlude and later recover their original shape. These processes point up the stability of the forecast calculation but also indicate the existence of other than just wave number three components in the flow field.

5. CONCLUSIONS

The primitive-equation barotropic forecast is highly sensitive to boundary conditions as well as to the finite-difference analog. The correct boundary conditions con-

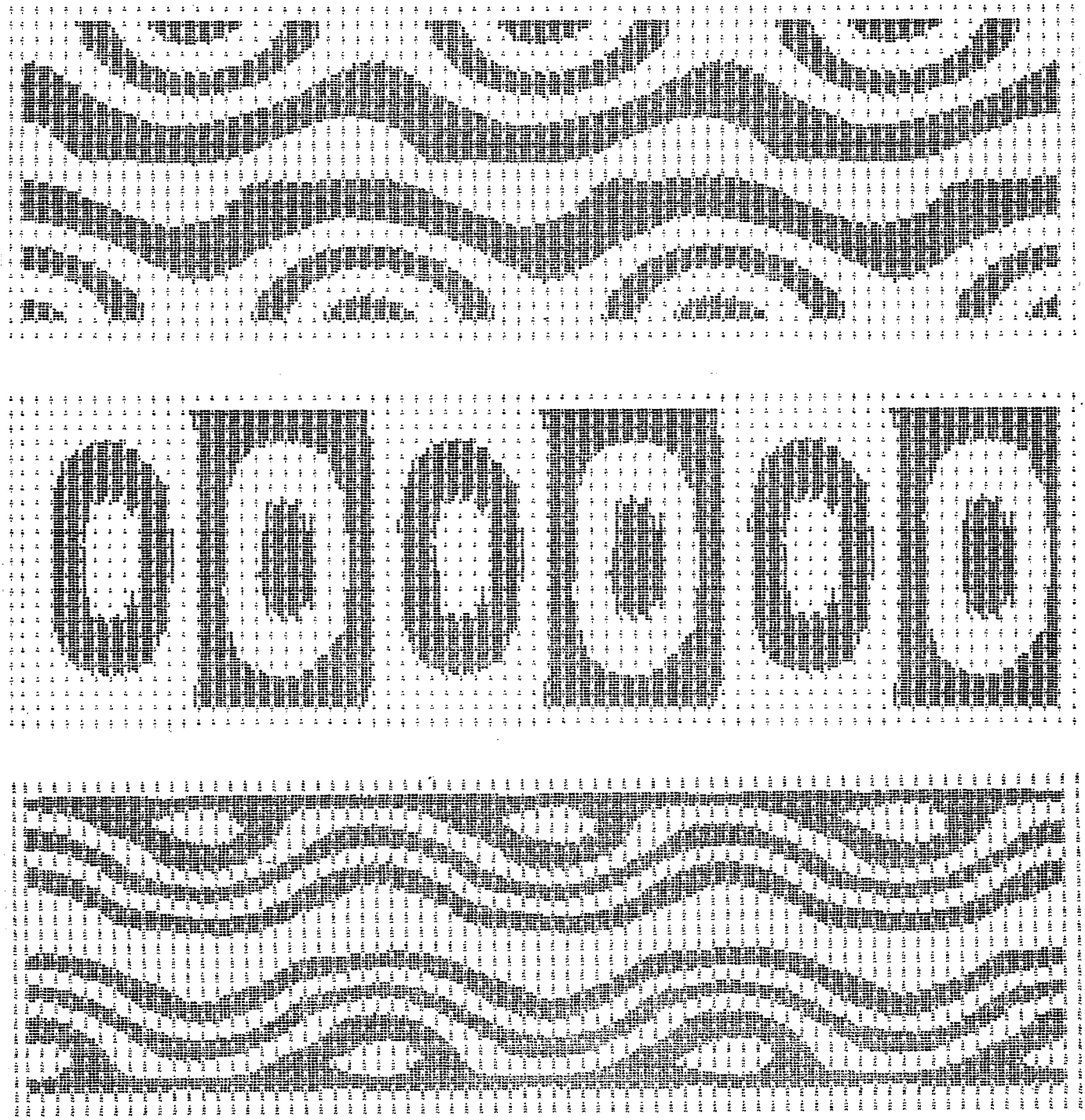

FIGURE 6.—Top, middle, and bottom maps are the 100-day forecast u, v, and h fields, respectively.

sistent with the difference systems are necessary to avoid contamination of the forecast by gravity waves and to allow successful long-period calculations. It appears that the generalized "semi-momentum" form, as given in equation (7), is viable indefinitely in extended integrations, when the boundary conditions are carefully formulated.

REFERENCE

1. F. G. Shuman, "Numerical Experiments with the Primitive Equations," *Proceedings of the International Symposium on Numerical Weather Prediction in Tokyo, November 7–13, 1960*, Meteorological Society of Japan, Mar. 1962, pp. 85–107.

[*Received December 1, 1965, revised March 24, 1966*]